Spiropyrans and spirooxazines
11.* Complexation of photochromic 5-(1,3-benzothiazol-2-yl)-substituted 1´,3´-dihydrospiro[benzo[*f*]chromene-3,2´-indole] with metal ions

I. A. Rostovtseva,[a] A. V. Chernyshev,[a] V. V. Tkachev,[b] S. M. Aldoshin,[b] N. A. Voloshin,[a] A. V. Metelitsa,[a] N. I. Makarova,[a] and V. I. Minkin[a]*

[a] *Institute of Physical and Organic Chemistry, Southern Federal University, 194/2 prosp. Stachki, 344090 Rostov-on-Don, Russian Federation. Fax: +7 (863 2) 43 4667. E-mail: photo@ipoc.sfedu.ru*
[b] *Institute of Problems of Chemical Physics, Russian Academy of Sciences, 1 prosp. Akad. Semenova, 142432 Chernogolovka, Moscow Region, Russian Federation. E-mail: sma@icp.ac.ru*

5-(1,3-Benzothiazol-2-yl)substituted 1´,3´-dihydrospiro[benzo[*f*]chromene-3,2´-indole] forms intensely colored complexes with metal ions in acetone solution in the absence of irradiation. The composition and stability of the complexes were shown to depend on the nature of the metal ion. The molecular structure of the zinc complex was determined by X-ray diffraction. The complexes with diamagnetic ions display negative photochromism associated with their reversible dissociation induced by visible light.

Key words: benzothiazole, spiropyrans, merocyanines, photochromism, complexation.

An alteration of the physicochemical properties of photochromic organic compounds due to reversible switching between two isomeric states induced by irradiation with UV or visible light is a rapidly developing area due to diverse fields of application, for example, as optical switches, materials for data storage, photochemically controlled chemical sensors, and so on.[2—4] Spiropyrans belong to one of the most well-studied classes of photochromic compounds due to wide possibilities of their structural modifications.[5,6] Polyfunctional molecular systems exhibiting, along with photochromism, light-switchable fluorescence,[7—11] magnetic,[12] and complexation[13—16] properties can be prepared by introducing various functional moieties into spiropyran molecules. Examples of such systems are azole-substituted spirochromenes[17—19] and spirobenzochromenes,[20—23] which exhibit luminescence properties in the spirocyclic form and are also capable of efficiently chelating transition metal ions. As a continuation of these studies, in the present work we investigated the complexation of spirobenzochromene containing the 1,3-benzothiazole substituent at position 5 of the benzochromene moiety.

Results and Discussion

An acetone solution of 5-benzothiazolyl-substituted spirobenzochromene (SBC) is substantially colored due to the presence of a small amount of the merocyanine isomer **B** in equilibrium with the spirocyclic isomer **A** (Scheme 1). The spirocyclic form is characterized by a long-wavelength absorption band with maxima at 386 and 405 nm ($\varepsilon_{386} = 5.41 \cdot 10^3$ L mol^{-1} cm^{-1} and $\varepsilon_{405} = 4.93 \cdot 10^3$ L mol^{-1} cm^{-1}).[22] The long-wavelength absorption band of the merocyanine isomer of SBC has a maximum at 613 nm.

The addition of equivalent amounts of Zn^{2+}, Cu^{2+}, Co^{2+}, and Ni^{2+} salts to acetone solutions of SBC in the absence of irradiation leads to the immediate intense coloration of the solutions due to the formation of the complexes $\mathbf{MB}_i$ of the merocyanine isomer of SBC (see Scheme 1). The visible spectral region shows intense absorption bands at 500—650 nm, the maxima of which are hypsochromically shifted with respect to the long-wavelength absorption band of the merocyanine form of SBC. A similar ionochromic effect was observed for SBC analogs, *viz.*, 8´-benzothiazolyl-substituted spirochromenes[17] and 5-benzoxazolyl-substituted SBC.[23] The addition of Mn^{2+} and Cd^{2+} salts results in the coloration of a solution of SBC if the metal salts are present in a 5—10-fold excess. Alkali and alkaline-earth metals do not cause the coloration even if they are present in a large excess.

The composition of the complexes was studied spectrophotometrically using the method of continuous variation (Job´s method),[24] which has been employed earlier to determine the compositions of similar complexes.[17,20,23,25]

* For Part 10, see Ref. 1.

Published in Russian in *Izvestiya Akademii Nauk. Seriya Khimicheskaya,* No. 3, pp. 0677—0682, March, 2015.

Scheme 1

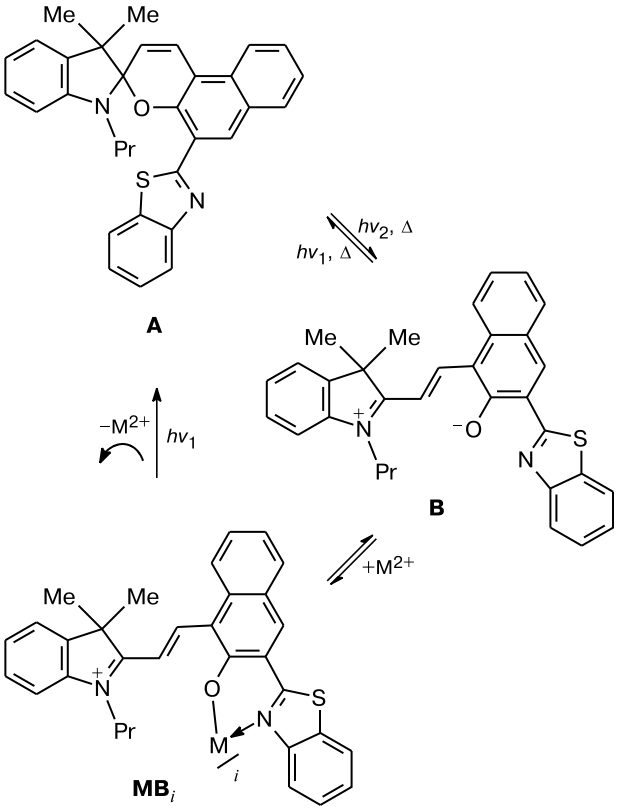

Note. hv_1 and hv_2 refer to irradiation with visible and UV light, respectively.

Figure 1 displays the isomolar diagram for SBC and $Zn(ClO_4)_2$ in acetone. A distinct extreme in the diagram corresponds to the equimolar composition (50 mol.% Zn and 50 mol.% SBC). The form of the diagram is independent of the observation wavelength. This attests to the formation of a 1 : 1 (metal : SBC) complex in solution. Similar data were obtained for Mn^{2+} and Cd^{2+} ions. In the case of Co^{2+}, Ni^{2+}, and Cu^{2+} ions, the isomolar diagrams show the formation of 1 : 2 complexes. Figure 2 depicts the isomolar diagram for SBC and $Ni(ClO_4)_2$ in acetone. The maximum in the diagram is shifted toward the lower metal content compared to the equimolar amount due to the contribution of both 1 : 1 and 1 : 2 (metal : SBC) complexes to the absorption at the observation wavelength.

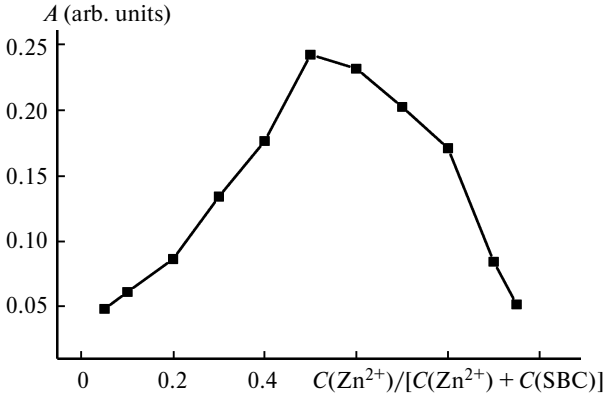

Fig. 1. Absorbance *versus* the composition of the isomolar series for SBC with zinc in acetone, $C(SBC) + C(Zn^{2+}) = 4 \cdot 10^{-5}$ mol L^{-1}, $\lambda_{app} = 567$ nm.

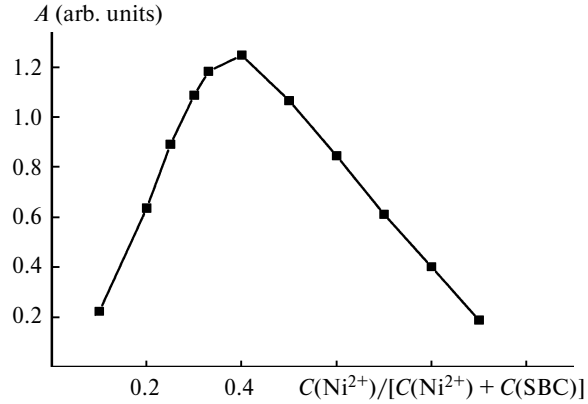

Fig. 2. Absorbance *versus* the composition of the isomolar series for SBC with nickel in acetone, $C(SBC) + C(Ni^{2+}) = 4 \cdot 10^{-5}$ mol L^{-1}, $\lambda_{app} = 607$ nm.

We obtained single crystals of the open form of SBC with zinc suitable for X-ray diffraction by the slow evaporation of the solvent from an acetone solution containing equimolar amounts of SBC and zinc chloride, which allowed us to study the molecular structure of this compound in detail. The composition of the complex in the solid state was found to be the same as in solution (1 : 1, zinc: SBC). The geometry of the complex in the crystal (X-ray diffraction study was performed at 150 K) is shown in Fig. 3 (atoms are represented as thermal ellipsoids drawn at 30% probability level).

A comparison of the structural details of the open forms of spiropyrans described earlier[26,27] and of the complex under study, which are related to the polymethine chain, including the indoline moiety and the phenolate oxygen atom, demonstrates that there are no changes in the structure of the open form of spiropyran upon the complexation. This refers both to the bipolar structure as a whole and the C(2′)—O(9′) bond lengths (1.282(5) Å). A similar situation was observed for the complex of antimony trichloride with the merocyanine form of 1′-isopropyl-8-methoxy-3′,3′-dimethyl-6-nitro-1′,3′-dihydrospiro-[chromene-2,2′-indole],[28] in which the coordination polyhedron can be described as a square pyramid.

The coordination polyhedron of Zn in the complex under study is a tetrahedron, with all angles at the zinc atom being in the range of 107.14(9)—118.06(9)°, except for the O(9′)—Zn(1)—N(3′) angle (91.6(1)°). This is apparently attributed to the fact that the distance between the O(9′) and N(3′) atoms in the molecule is 2.833(5) Å due to the necessity of the six-membered metallocycle

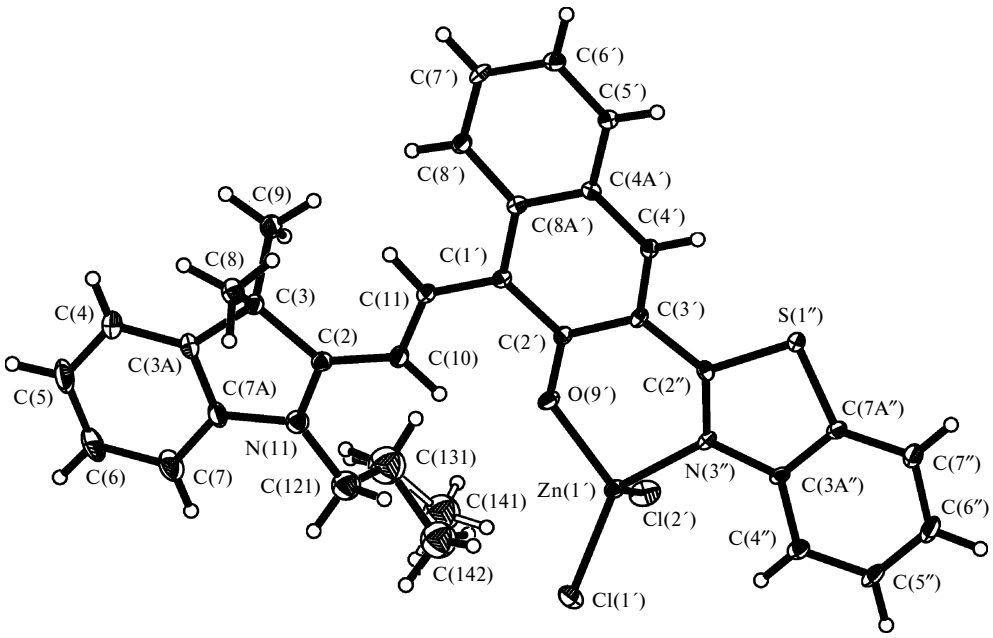

Fig. 3. Molecular structure of the complex of SBC with zinc.

closure because all angles at the carbon, nitrogen, and oxygen atoms of the metallocycle are in the range of 122.0(3)—127.4(3)°. The C(8)—C(9)—C(1′) (129.4(4)°) and N(3)—C(2)—C(10) (127.4(3)°) angles are also larger than 120° due apparently to steric factors as well. Thus, the distance between the H(8) and O(9′) atoms is 2.03 Å, which is undoubtedly associated with the coordination of zinc by the O(9′) and N(3″) atoms. A similar distortion of the tetrahedral environment of the zinc atom involving two chlorine, one oxygen, and one nitrogen atoms was observed in the zinc complex with the oxazole-containing ligand,[29] in which the O...N distance is 3.04 Å, and the O—Zn—N and Cl—Zn—Cl angles are 95.6 and 123.0°, respectively; the other angles in the tetrahedron are in the range of 102—113°. For comparison, it may be noted that the coordination polyhedron of BF_2 in the complex of 4-(4-chlorophenyl)-1,1-difluoro-3-methyl-1*H*-pyrido-[1,2-*c*][1,3,2]oxazaborinin-9,1-ylide is also a tetrahedron,[30] but the N...O distance is 2.477(6) Å and the angles at the boron atom are in the range of 106.6—110.6°.

The terminal atom of the propyl group in the complex under study is disordered over two positions with an occupancy ratio of 2 : 1 (the less occupied position is not dashed).

The important characteristics of complexes in solution are their stability constants. The formation of SBC complexes with metal ions in solution (see Scheme 1) can be represented as a combination of coupled equilibria:

$$\mathbf{A} \rightleftharpoons \mathbf{B},$$

$$\mathbf{B} + \mathbf{M} \rightleftharpoons \mathbf{MB},$$

$$\mathbf{B} + \mathbf{MB} \rightleftharpoons \mathbf{MB}_2.$$

These equilibria are characterized by the following constants:

$$K_T = [\mathbf{B}]/[\mathbf{A}], \quad (1)$$

$$K_1 = [\mathbf{MB}]/([\mathbf{B}][\mathbf{M}]), \quad (2)$$

$$K_2 = [\mathbf{MB}_2]/([\mathbf{MB}][\mathbf{M}]). \quad (3)$$

Spirobenzochromene in acetone is characterized by a low equilibrium content of the merocyanine isomer, which cannot be quantified by NMR spectroscopy.[31] Consequently, the constant K_T cannot be calculated. For this reason, the evaluation of the true stability constants of the merocyanine form with metal ions (see Eqs (2) and (3)) is hindered. Besides, the equilibrium constants (2) and (3) cannot be determined by the method proposed in the study[32] because of the very short (<1 s)[22] relaxation time of the merocyanine isomer at $T = 293$. Therefore, we calculated the effective stability constants, which account for the tautomeric equilibrium of the ligand:[20]

$$K_i^{\text{eff}} = [\mathbf{MB}_i]/([\mathbf{MB}_{i-1}][\mathbf{L}]^i), \quad (4)$$

where $[\mathbf{L}] = [\mathbf{B}] + [\mathbf{A}] = C_{\mathbf{L}} - \sum_i i[\mathbf{MB}_i]$ is the equilibrium concentration of the SBC forms, which are not involved in the complex, and $C_{\mathbf{L}}$ is the total concentration of SBC. It is the values of K_i^{eff} that are required for practical calculations of the degree of complexation and the prediction of the strength of the binding of metal ions in complexes under real conditions, which is impor-

tant for the application of these compounds for analytical purposes.

The stability constants K_i^{eff} were determined spectrophotometrically based on the dependences of the absorbance of solutions containing a fixed amount of SBC and a variable amount of the metal salt.

In the case when SBC forms only a 1 : 1 complex with a metal ion, the absorption spectra show a single band of the complex in the visible region (Fig. 4), and the concentration dependence of the absorbance can be described by Eq. (5):[33]

$$A = A_0 + [(A_{\max} - A_0)/(2C_{\mathbf{L}})]\{C_{\mathbf{L}} + C_{\mathbf{M}} + 1/K_i^{\text{eff}} - \\ - [(C_{\mathbf{L}} + C_{\mathbf{M}} + 1/K_i^{\text{eff}})^2 - 4C_{\mathbf{L}}C_{\mathbf{M}}]^{1/2}\}. \quad (5)$$

Figure 4 depicts the absorption spectra of SBC in the presence of cadmium ions, which are indicative of the formation of 1 : 1 complexes. Figure 5 presents the absorption spectra of SBC containing different amounts of cobalt ions. As can be seen in Fig. 5, the intensity and position of the long-wavelength absorption maximum largely depends on the amount of the metal salt in solution, resulting from the formation of both 1 : 1 and 1 : 2 complexes. Solutions *1*—*6* containing an excess of SBC are characterized by the predominance of the 1 : 2 complex. The visible region of the absorption spectra shows a maximum at 606 nm. An increase in the metal concentration (solutions *7*—*13*) up to the 15-fold excess leads to a decrease in the percentage of the 1 : 2 complex and an increase in the percentage of the 1 : 1 complex, which is manifested in the spectra as a decrease in the absorption at 600 nm and the appearance of a new band with a maximum at 578 nm. In this case, the calculation of the stability constants is based on the iterative numerical solution of the system of Eqs (6)—(10) by the minimization of the function

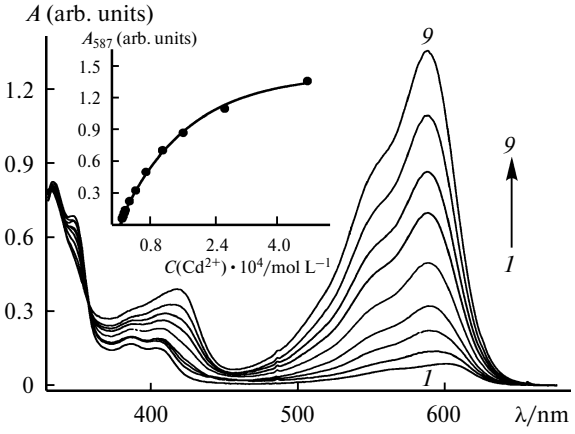

Fig. 4. Changes in the absorption spectrum of SBC upon the addition of different amounts of $Cd(ClO_4)_2$ in acetone; $C(\text{SBC}) = 2.45 \cdot 10^{-5}$ mol L^{-1}; $C(Cd^{2+}) = 2.14 \cdot 10^{-6}$ (*1*), $8.54 \cdot 10^{-6}$ (*2*), $1.71 \cdot 10^{-5}$ (*3*), $2.99 \cdot 10^{-5}$ (*4*), $5.12 \cdot 10^{-5}$ (*5*), $8.54 \cdot 10^{-5}$ (*6*), $1.28 \cdot 10^{-4}$ (*7*), $2.14 \cdot 10^{-4}$ (*8*), and $3.84 \cdot 10^{-4}$ mol L^{-1} (*9*). The inset shows the dependence of the absorbance in the absorption maximum of the complex (at 587 nm) on the Cd^{2+} concentrations; the points correspond to the experimental data, and the solid curves represent the calculated data.

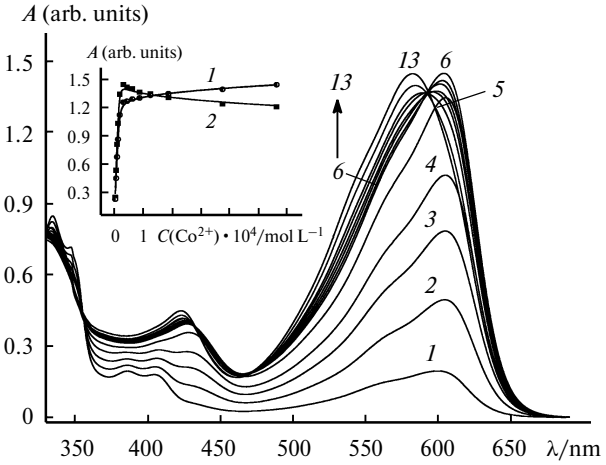

Fig. 5. Changes in the absorption spectrum of SBC upon the addition of different amounts of $Co(ClO_4)_2$ in acetone; $C(\text{SBC}) = 3.66 \cdot 10^{-5}$ mol L^{-1}; $C(Co^{2+}) = 3.14 \cdot 10^{-6}$ (*1*), $6.28 \cdot 10^{-6}$ (*2*), $9.42 \cdot 10^{-6}$ (*3*), $1.26 \cdot 10^{-5}$ (*4*), $1.88 \cdot 10^{-5}$ (*5*), $3.14 \cdot 10^{-5}$ (*6*), $4.39 \cdot 10^{-5}$ (*7*), $6.28 \cdot 10^{-5}$ (*8*), $8.79 \cdot 10^{-5}$ (*9*), $1.26 \cdot 10^{-4}$ (*10*), $1.88 \cdot 10^{-4}$ (*11*), $3.77 \cdot 10^{-4}$ (*12*), and $5.65 \cdot 10^{-4}$ mol L^{-1} (*13*). The inset shows the dependence of the absorbance at 582 (*1*) and 603 nm (*2*) on the Co^{2+} concentration; the points correspond to the experimental data, and the solid curves represent the calculated data.

$$F = \sum_{i=1}^{n_S} \sum_{j=1}^{n_\lambda} (A_{\text{app}} - A_{\text{calc}})^2 \rightarrow \min,$$

where n_S is the number of solutions and n_λ is the number of the observation wavelengths.

$$A_{\text{calc}} = \varepsilon_{\mathbf{ML}}[\mathbf{MB}] + \varepsilon_{\mathbf{ML2}}[\mathbf{MB_2}] + \varepsilon_{\mathbf{L}}^{\text{eff}}[\mathbf{L}] + \varepsilon_{\mathbf{M}}[\mathbf{M}] \quad (6)$$

$$[\mathbf{MB}] = C_{\mathbf{M}}K_1^{\text{eff}}[\mathbf{L}]/(1 + K_1^{\text{eff}}[\mathbf{L}] + K_1^{\text{eff}}K_2^{\text{eff}}[\mathbf{L}]^2) \quad (7)$$

$$[\mathbf{MB_2}] = C_{\mathbf{M}}K_1^{\text{eff}}K_2^{\text{eff}}[\mathbf{L}]^2/(1 + K_1^{\text{eff}}[\mathbf{L}] + \\ + K_1^{\text{eff}}K_2^{\text{eff}}[\mathbf{L}]^2) \quad (8)$$

$$C_{\mathbf{L}} = [\mathbf{MB}] + 2[\mathbf{MB_2}] + [\mathbf{L}] \quad (9)$$

$$C_{\mathbf{M}} = [\mathbf{MB}] + [\mathbf{MB_2}] + [\mathbf{M}] \quad (10)$$

Figure 5 also depicts the experimental dependences of the absorbance at the chosen wavelengths on the concentration of the metal ion. These dependences are in good agreements with the theoretically calculated values (solid curves). The stability constants of the complexes and their absorption spectroscopic characteristics are given in Table 1. The stability of the complexes increases in the

Table 1. Calculated logarithms of the effective complex formation constants and absorption spectroscopic characteristics of the SBC complexes in acetone; $T = 293$ K

Metal	**MB**			**MB_2**		
	$\log K_1^{eff}$	λ_{max} /nm	$\varepsilon_{max} \cdot 10^{-3}$ /L mol^{-1} cm^{-1}	$\log K_2^{eff}$	λ_{max} /nm	$\varepsilon_{max} \cdot 10^{-3}$ /L mol^{-1} cm^{-1}
Cd	3.92±0.01	587	51.6	—	—	—
Zn	5.85±0.01	572	44.7	—	—	—
Co	5.5±0.1	578	45.5	6.6±0.1	606	82.3
Cu	7.2±0.5	562	32.9	6.1±0.5	574	50.3
Mn	3.18±0.01	585	33.5	—	—	—
Ni	6.0±0.5	585	51.3	7.3±0.5	607	101.6

series of Mn^{2+}, Cd^{2+}, Zn^{2+}, Co^{2+}, Ni^{2+}, Cu^{2+} ions. The absorption bands of the 1 : 2 complexes are bathochromically shifted with respect to the absorption bands of the 1 : 1 complexes and have a 1.5—2 times higher intensity.

The visible light irradiation of solutions of the SBC complexes with diamagnetic cadmium and zinc ions leads to thermal decoloration due to the photodissociation to the initial spirocyclic isomer and free metal ions. After the switching-off of the radiation source, the initial equilibrium is recovered. Complexes with paramagnetic ions are resistant to radiation. The quantum yield is a quantitative parameter characterizing the efficiency of the photoprocess. This parameter was calculated using the photostationary state approximation. For this purpose, a solution of SBC in the presence of an excess of a metal salt was irradiated with filtered visible light (λ = 546 or 578 nm) in order to completely transform SBC into the corresponding complex, and the absorption spectra were simultaneously recorded until the photostationary state was achieved (Fig. 6). Based on the results of this study, the molar fraction of the complex in the photostationary state was determined from the relation $\alpha_{st} = A_{st}/A_0$, where A_{st} is the absorbance of the solution in the absorption maximum

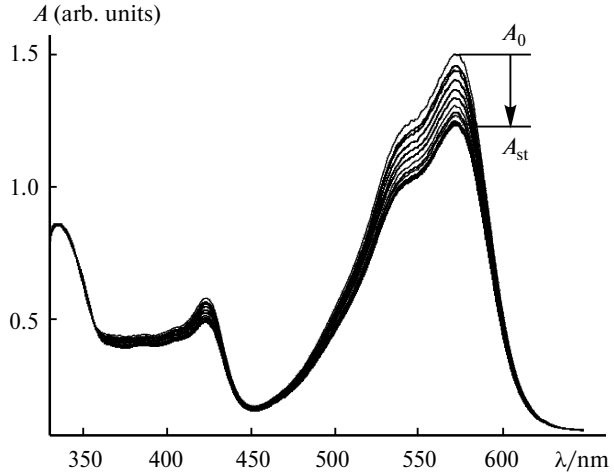

Fig. 6. Changes in the absorption spectrum of the SBC complex with zinc ions upon irradiation with visible light at λ = 578 nm.

Table 2. Photodissociation quantum yields of the complexes at λ = 546 (I) and 578 nm (II)

Metal	$\Phi \cdot 10^3$	
	I	II
Cd	3.3	2.9
Zn	6.5	5.3

of the complex in the photostationary state and A_0 is the absorbance of the solution before irradiation. The quantum yield was calculated by the equation[23]

$$\Phi = k_\Delta(1 - \alpha_{st})C_0/\{[1 - \exp(-2.303A_{max}\alpha_{st})]I_0\}.$$

The calculated values are in the range of 0.0029—0.0065 (Table 2) and are virtually independent of the radiation wavelength.

Therefore, 5-(1,3-benzothiazol-2-yl)-substituted 1´,3´-dihydrospiro[benzo[*f*]chromene-3,2´-indole] exhibits ionochromic properties due to the formation of intensely colored stable complexes of the merocyanine isomer with transition metal ions. The composition and stability of the complexes are determined by the nature of the central ion. The complexes with zinc and cadmium ions display negative photochromism due to photodissociation.

Experimental

The synthesis of spirobenzochromene has been described earlier.[22] The electronic absorption spectra and the kinetic curves were recorded on an Agilent 8453 spectrophotometer equipped with a temperature-control accessory. The photolysis of solutions was performed by irradiation with a Newport system based on a 200 W mercury lamp equipped with interference filters. Solutions were prepared using acetone of spectrophotometric grade (Aldrich). The optical radiation intensity, which was determined with a Newport 2935 optical power meter at the wavelengths of 546 and 578 nm, was $1.8 \cdot 10^{17}$ and $1.9 \cdot 10^{17}$ photon s^{-1}, respectively.

X-ray diffraction study. The unit cell parameters were determined and the three-dimensional set of intensities was measured on a Xcalibur, Eos automated diffractometer (Mo-Kα radiation,

graphite monochromator) at 150 K. Black single crystals of the complex $C_{32}H_{28}N_2OCl_2SZn$ (M = 624.89) are monoclinic, a = = 9.7805(5) Å, b = 29.2694(16) Å, c = 10.2480(5) Å, β = 93.375(4)°, V = 2928.6(3) Å^3, Z = 4, d_{calc} = 1.417 g cm^{-3}, μ(Mo-Kα) = = 1.121 mm^{-1}, space group $P2_1/c$. The intensities of 17452 reflections were measured in the angle range 2θ ≤ 59.0° using the ω-scanning technique from a single crystal of dimensions 0.40×0.30×0.25 mm. The empirical absorption correction was applied using the Multiscan technique. After rejection of systematic absences and merging of equivalent reflections (R(int) = 0.018), the X-ray data set contained 8088 unique reflections ($F^2(hkl)$ and $\sigma(F^2)$), of which 6749 reflections were with $F^2 > 2\sigma(F^2)$. The structure was solved by direct methods and refined by the full-matrix least-squares method based on F^2 using the SHELXTL program package with anisotropic displacement parameters for nonhydrogen atoms, except for the less occupied C(142) atom (see Fig. 3). Attempts to refine the latter atom with an anisotropic displacement parameter revealed the further disorder of the atoms of the propyl group. In the crystal structure of the complex under study, most of H atoms were located in difference Fourier maps, and then the coordinates and isotropic thermal parameters for all H atoms were refined by the least-squares method using a riding model.[34] In the last cycle of the full-matrix refinement, the absolute shifts of all 352 variable parameters of the structure were 0.003σ. The final refinement parameters were R_1 = 0.081, R_w = 0.15; GOOF = 1.247 based on the observed reflections. After the refinement, the maximum and minimum difference electron densities were 1.789 and −0.772 e A^{-3}, respectively. The CIF file, which contains the complete information on the structure, was deposited in the Cambridge Crystallographic Data Centre (CCDC 1039032) and can be obtained, free of charge, on application to www.ccdc.cam.ac.uk/data_request/cif. In conclusion, let us note that we treated the quite pronounced residual electron density maximum as an indication of the presence of a water molecule. The refinement of the occupancy of this water molecule gave 0.25. However, taking into account an insignificant decrease in the R factor (0.003) and the absence of possible hydrogen bonds, this assumption cannot be made with confidence.

This study was financially supported by the Russian Foundation for Basic Research (Project No. 12-03-33112 mol_a_ved).

References

1. N. A. Voloshin, A. V. Chernyshev, E. V. Solov´eva, I. A. Rostovtseva, A. V. Metelitsa, G. S. Borodkin, V. A. Kogan, V. I. Minkin, *Russ. Chem. Bull.* (*Int. Ed.*), 2014, **63**, 1373 [*Izv. Akad. Nauk, Ser. Khim.*, 2014, 1373].
2. *Molecular Switches*, Eds B. L. Feringa, W. R. Browne, Wiley, Weinheim, 2011, 2nd ed., Vol. **1**, **2**.
3. R. C. Bertelson, in *Organic Photochromic and Thermochromic Compounds. Topics in Applied Chemistry*, Eds J. C. Crano, R. J. Guglielmetti, Plenum Press, New York, 1999, Vol. **1**, p. 11.
4. V. I. Minkin, *Russ. Chem. Rev.*, 2013, **82**, 1.
5. V. I. Minkin, *Chem. Rev.*, 2004, **104**, 2751.
6. R. Klajn, *Chem. Soc. Rev.*, 2014, **43**, 148.
7. V. A. Barachevsky, *J. Fluorescence*, 2000, **10**, 185.
8. S. A. Ahmed, M. Tanaka, H. Ando, K. Tawa, K. Kimura, *Tetrahedron*, 2004, **60**, 6029.
9. J.-R. Chen, J.-B. Wong, P.-Y. Kuo, D.-Y. Yang, *Org. Lett.*, 2008, **10**, 4823.
10. M. Tomasulo, E. Deniz, R. J. Alvarado, F. M. Raymo, *J. Phys. Chem. C*, 2008, **112**, 8038.
11. B. Seefeldt, R. Kasper, M. Beining, J. Mattay, J. Arden-Jacob, N. Kemnitzer, K. H. Drexhage, M. Heilemann, M. Sauer, *Photochem. Photobiol. Sci.*, 2010, **9**, 213.
12. S. M. Aldoshin, *J. Photochem. Photobiol. A: Chem.*, 2008, **200**, 19.
13. S. Kum, H. Nishihara, *Struct. Bond.*, 2007, **123**, 79.
14. S. V. Paramonov, B. V. Lokshin, O. A. Fedorova, *J. Photochem. Photobiol. C: Photochem. Rev.*, 2011, **12**, 209.
15. M. Natali, S. Giordani, *Chem. Soc. Rev.*, 2012, **41**, 4010.
16. V. A. Barachevsky, *Rev. J. Chem.*, 2013, **3**, 52 [*Obzor. Zh. Khim.*, 2013, **3**, 58].
17. M. I. Zakharova, C. Coudret, V. Pimienta, J. C. Micheau, S. Delbaere, G. Vermeersch, A. V. Metelitsa, N. A. Voloshin, V. I. Minkin, *Photochem. Photobiol. Sci.*, 2010, **9**, 199.
18. J. Q. Ren, H. Tian, *Sensors*, 2007, **7**, 3166.
19. M. Natali, L. Soldi, S. Giordani, *Tetrahedron*, 2010, **66**, 7612.
20. A. V. Chernyshev, N. A. Voloshin, I. M. Raskita, A. V. Metelitsa, V. I. Minkin, *J. Photochem. Photobiol. A: Chem.*, 2006, **184**, 289.
21. N. A. Voloshin, A. V. Chernyshev, A. V. Metelitsa, V. I. Minkin, *Chem. Heterocycl. Compd.* (*Engl. Transl.*), 2011, **47**, 865 [*Khim. Geterotsikl. Soedin.*, 2011, 1055].
22. N. A. Voloshin, A. V. Chernyshev, A. V. Metelitsa, E. B. Gaeva, V. I. Minkin, *Russ. Chem. Bull.* (*Int. Ed.*), 2011, **60**, 1921 [*Izv. Akad. Nauk, Ser. Khim.*, 2011, 1888].
23. A. V. Chernyshev, N. A. Voloshin, A. V. Metelitsa, V. V. Tkachev, S. M. Aldoshin, E. Solov´eva, I. A. Rostovtseva, V. I. Minkin, *J. Photochem. Photobiol. A: Chem.*, 2013, **265**, 1.
24. E. Bruneau, D. Lavabre, G. Levy, J. C. Micheau, *J. Chem. Educ.*, 1992, **69**, 833.
25. M. Natali, C. Aakeroy, J. Desper, S. Giordani, *Dalton Trans.*, 2010, **39**, 8269.
26. X. Guo, Y. Zhou, D. Zhang, B. Yin, Zh. Liu, C. Liu, Zh. Lu, Yu. Huang, Da. Zhu, *J. Org. Chem.*, 2004, **69**, 8924.
27. N. K. Artemova, V. A. Smirnov, B. G. Rogachev, G. V. Shilov, S. M. Aldoshin, *Russ. Chem. Bull.* (*Int. Ed.*), 2006, **55**, 1605 [*Izv. Akad. Nauk, Ser. Khim.*, 2006, 1548].
28. E. A. Shilova, A. Samat, G. Pèpe, *Zeitschr. Kristallogr. — New Cryst. Struct.*, 2011, **226,** 71.
29. H. Wamhoff, N. Horlemann, Zhu Nai-jue, G. Fang, *Chem. Zeit.*, 1986, **110**, 315.
30. M. Froimowitz, Y. Gu, L. A. Dakin, C. J. Kelley, D. Parrish, J. R. Deschamps, *Bioorg. Med. Chem. Lett.*, 2005, **15**, 3044.
31. N. A. Voloshin, A. V. Chernyshev, A. V. Metelitsa, S. O. Bezuglyi, E. N. Voloshina, V. I. Minkin, *Russ. Chem. Bull.* (*Int. Ed.*), 2008, **57**, 151 [*Izv. Akad. Nauk, Ser. Khim.*, 2008, 146].
32. M.Kubinyi, O. Varga, P. Baranyai, M. Kőllay, R. Miszei, G. Tárkányi, T. Vidoczy, *J. Mol. Struct.*, 2011, **1000**, 77.
33. J. Bourson, J. Pouget, B. Valeur, *J. Phys. Chem.*, 1993, **97**, 4552.
34. G. M. Sheldrick, *SHELXTL v. 6.14*, *Structure Determination Software Suite*, Bruker AXS, Madison, Wisconsin, USA, 8/06/2000.

Received December 11, 2014;
in revised form February 3, 2015